Novel Peptide Nucleic Acid That Shows High Sequence Specificity and All-or-None-Type Hybridization with the Complementary DNA

Masayasu Kuwahara, Miki Arimitsu, and Masahiko Sisido*

Department of Bioscience and Biotechnology
Faculty of Engineering, Okayama University
3-1-1 Tsushimanaka, Okayama 700-8530, Japan

Received June 11, 1998

Peptide nucleic acids (PNAs) have been attracting interest as the antisense molecules that resist degradation by nucleases or proteases. Nielsen and co-workers have been reporting PNAs with a [NH-CH_2-CH_2-N(CO-CH_2-Base)-CH_2-CO] monomer unit (**III** in Chart 1 with adeninyl base).[1] The PNAs bind to the complementary DNAs with higher affinity than the corresponding DNA−DNA mixture. After the Nielsen's PNA, several workers reported PNAs of different main chain structures,[2] aiming to improve the limited solubility and other drawbacks of the Nielsen's PNA.[3] However, most of these new PNAs showed little interaction with nucleic acids, indicating that the detailed molecular structure of the PNAs plays a crucial role in the hybridization with nucleic acids.

In this paper, we report a novel PNA (oxy-PNA = OPNA) with a monomer unit [NH-C*H(CH_2-CH_2-Base)-CH_2-O-CH_2-CO] (**II** in Chart 1 with adeninyl group) and its strong hybridization with DNAs. The OPNA has an ether linkage in the main chain that improved water solubility. The most advantageous point of the OPNA is its all-or-none-type hybridization that enables detection of even single mismatched DNAs.

The Fmoc-protected δ-amino acids with N^6-benzoyladenine, thymine, uracil, and N^4-benzoylcytosine were prepared through an eight-step synthesis starting from L-homoserine.[4] The Fmoc δ-amino acids were linked together through solid-phase peptide synthesis to prepare OPNA(A_{12}) (**II**).[5] Details are described in Supporting Information. The solubility of the OPNA(A_{12}) in pure water was 0.64 base M. The Nielsen-type PNA with 12 adeninyl units [**III**, PNA(A_{12})] was also prepared.[6] The solubility of PNA(A_{12}) was 0.33 base M.

As indicated on the right ordinate of Figure 1, the OPNA(A_{12}) showed virtually no CD signal at the absorption band of adenine unit, indicating the absence of helical conformation in the single-stranded form, probably because of the flexibility of the OPNA main chain.

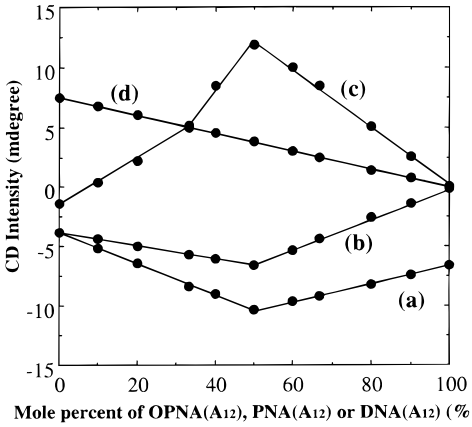

Figure 1. Job plots for CD intensities of the mixtures of (a) DNA(A_{12})−DNA(T_{12}) (at 249 nm), (b) OPNA(A_{12})−DNA(T_{12}) (at 249.5 nm), (c) PNA(A_{12})−DNA(T_{12}) (at 261 nm), and (d) OPNA(A_{12})−DNA(C_{12}) (at 277 nm), in 150 mM NaCl, 10 mM NaH_2PO_4, and 0.1 mM EDTA at pH 7.0 and 5 °C. Total base concentration = 270 μM. Optical path length = 2 mm.

Chart 1

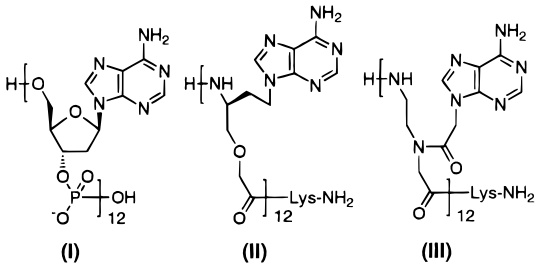

UV absorption and CD spectra were measured for mixtures of OPNA(A_{12}) and DNA(T_{12}) at different molar ratios. Figure 1 shows plots of CD intensities against the molar ratios. The Job plot showed a minimum at 1/1 molar ratio. In contrast, no minimum or maximum was observed for mixtures of OPNA(A_{12})−DNA(C_{12}), indicating sequence specific interactions between OPNA and DNA. Similar Job plots were observed for the Nielsen's PNA(A_{12})−DNA(T_{12}) and for the DNA(A_{12})−DNA(T_{12}) mixtures. In the case of PNA(A_{12})−DNA(T_{12}), however, the Job plot shows a turning point at PNA/DNA ≈ 1/2, suggesting a presence of some unknown structure. These spectroscopic results strongly suggest sequence specific hybridization of OPNA(A_{12}) with DNA(T_{12}).

Temperature dependence of the absorption intensity of the OPNA(A_{12})/DNA(T_{12}) (1/1) mixture at 260 nm is shown in Figure 2, together with those for the Nielsen's PNA(A_{12})/DNA(T_{12}) (1/1) mixture and for the DNA(A_{12})−DNA(T_{12}) (1/1) mixture. A very sharp transition was observed for the OPNA(A_{12})−DNA(T_{12}) mixture as compared with other two cases. The temperature ranges for 5−95% transition are 15° for the OPNA(A_{12}), 29.5° for the PNA(A_{12}), and 18.5° for the DNA(A_{12}), respectively. The transition temperature (T_m) for the OPNA(A_{12})−DNA(T_{12}) complex (43 °C) is higher than that for the DNA(A_{12})−DNA(T_{12}) complex (30 °C) but lower than that for the PNA(A_{12})−DNA(T_{12}) complex (55 °C).

The details of the transition may be discussed in terms of the thermodynamic analysis of the melting curve.[7] The temperature dependence of the association constants for the three mixtures

* Corresponding author: Tel: +81-86-251-8218. Fax: +81-86-251-8219. E-mail: sisido@cc.okayama-u.ac.jp.

(1) (a) Nielsen, P. E.; Egholm, M.; Berg, R. H.; Buchardt, O. *Science* **1991**, *254*, 1497. (b) Egholm, M.; Buchardt, O.; Christensen, L.; Behrens, C.; Freier, S. M.; Driver, D. A.; Berg, R. H.; Kim, S. K.; Nordén, B.; Nielsen, P. E. *Nature* **1993**, *365*, 566. (c) Wittung, P.; Nielsen, P. E.; Buchardt, O.; Egholm, M.; Nordén, B. *Nature* **1994**, *368*, 561. (d) Bohler, C.; Nielsen, P. E.; Orgel, L. E. *Nature* **1995**, *376*, 578. (e) Veselkov, A. G.; Demidov, V. V.; Frank-Kamenetiskii, M. D.; Nielsen, P. E. *Nature* **1996**, *379*, 214.

(2) (a) Almarsson, Ö.; Bruice, T. C.; Kerr, J.; Zuckermann, R. N. *Proc. Natl. Acad. Sci. U.S.A.* **1993**, *90*, 7818. (b) Hyrup, B.; Egholm, M.; Nielsen, P. E.; Wittung, P.; Nordén, B.; Buchardt, O. *J. Am. Chem. Soc*. **1994**, *116*, 7964. (c) Gangamani, B. P.; Kumar, V. A.; Ganesh, K. N. *Tetrahedron* **1996**, *52*, 15017. (d) Tsantrizos, Y. S.; Lunetta, J. F.; Boyd, M.; Fader, L. D.; Wilson, M.-C. *J. Org. Chem*. **1997**, *62*, 5451. (g) Ciapetti, P.; Soccolini, F.; Taddei, M. *Tetrahedron* **1997**, *53*, 1167. (f) Lowe, G.; Vilaivan, T. *J. Chem. Soc., Perkin Trans. 1* **1997**, *4*, 539 (g) Efimov, V. A.; Choob, M. V.; Buryakova, A. A.; Kalinkina, A. L.; Chakhmakhcheva, O. G. *Nucleic Acids Res*. **1998**, *26*, 566.

(3) Manufacturer's guidline; PerSptive Biosystems, Framingham, MA, 1995.

(4) FAB MS (JEOL JMS-DX303) data of the Fmoc-protected δ-amino acids bearing N^6-benzoyladenine, thymine, uracil, and N^4-benzoylcytosine: 607.2291 (M + H^+, calcd for $C_{33}H_{31}N_6O_6$ 607.2305), 494.1929 (M + H^+, calcd for $C_{26}H_{28}N_3O_7$ 494.1927), 480.1797 (M + H^+, calcd for $C_{25}H_{26}N_3O_7$ 480.1771), and 583.2204 (M + H^+, calcd for $C_{32}H_{31}N_4O_7$ 583.2193), respectively.

(5) MALDI-TOF MS (Finnigan Vision 2000) data of the OPNA(A_{12}): *m*/*z* 3295.7 (M + H^+, calcd 3292.7).

(6) MALDI-TOF MS data of the PNA(A_{12}): *m*/*z* 3465.3 (M + Na^+, calcd 3469.4).

10.1021/ja9820386 CCC: $18.00
Published on Web 12/19/1998

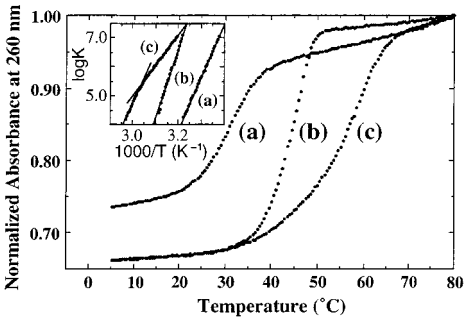

Figure 2. Temperature dependence of absorption intensity at 260 nm for equimolar mixtures of (a) DNA(A_{12})−DNA(T_{12}), (b) OPNA(A_{12})−DNA(T_{12}), and (c) PNA(A_{12})−DNA(T_{12}) in 150 mM NaCl, 10 mM NaH_2PO_4, and 0.1 mM EDTA, pH 7.0. Duplex concentration = 5.9 μM. The melting curves were recorded at the interval of 0.5°/0.5 min. Insert shows the van't Hoff plots of the association constants.

Table 1. Thermodynamic Parameters for the Hybridizations of the Mixtures of DNA(A_{12}), OPNA(A_{12}), and PNA(A_{12}) with DNA(T_{12}) or DNA(T_6CT_5)

components	T_m (°C)	ΔH (kcal mol^{-1})	ΔS (cal mol^{-1} K^{-1})
Full Matching			
DNA(A_{12})−DNA(T_{12})	30	-83.7 ± 3.0[a]	-251 ± 10[a]
OPNA(A_{12})−DNA(T_{12})	43	-112 ± 0.1	-329 ± 0.2
PNA(A_{12})−DNA(T_{12})	55	-47.7 ± 0.2	-120 ± 0.5[b]
		-79.5 ± 4.3	-217 ± 1.3[c]
Single Mismatching			
DNA(A_{12})−DNA(T_6CT_5)	12	-70.5 ± 6.7	-222 ± 23
OPNA(A_{12})−DNA(T_6CT_5)	30	-97.7 ± 0.1	-297 ± 0.2
PNA(A_{12})−DNA(T_6CT_5)	42	-59.0 ± 5.5	-161 ± 17[b]
		-77.3 ± 3.0	-220 ± 9.0[c]

[a] Error ranges are estimated from the variations in the baselines of the melting curves. [b] Taken from the low-temperature side of the van't Hoff plot. [c] Taken from the high-temperature side of the van't Hoff plot.

are shown in the insert of Figure 2. The van't Hoff plots for the DNA(A_{12})−DNA(T_{12}) mixture and for the OPNA(A_{12})−DNA(T_{12}) mixture are straight over the whole range of the transition, indicating a single-step transition. On the other hand, the plot for the PNA(A_{12})−DNA(T_{12}) mixture shows a turning point that may suggest the presence of some unknown structure that coexists with the double-stranded form.

Thermodynamic parameters evaluated from the van't Hoff plot are listed in Table 1. Both the changes in the stabilizing energy ($-\Delta H$) and the conformational constraints ($-\Delta S$) are largest in the OPNA(A_{12})−DNA(T_{12}) pair, suggesting that, by decreasing temperature, the randomly coiled OPNA with large conformational entropy is folded into a regular and rigid double-stranded helix with nearly optimized stabilization energy.

The single step transition for the OPNA(A_{12})−DNA(T_{12}) mixture was confirmed by CD spectroscopy. The CD spectra measured at varying temperatures showed a gradual change from the profile for the double-stranded form to that for the single-stranded form with several isodichroic points. The isodichroic points indicate that the transition is occurring without any intermediate state. In contrast to this, the CD for the Nielsen's PNA(A_{12})−DNA(T_{12}) pair showed a complex change during the gradual rise of temperature. The complex behavior of the Nielsen's PNA has been also suggested from the curvature in the CD Job plot (Figure 1). The complex behavior of the Nielsen's PNA-(A_{12})−DNA(T_{12}) mixture indicates the presence of some unknown structure such as a triplex, that coexists with the simple duplex.

It must be noted that the double-stranded structure and the hybridization thermodynamics for the DNA(A_{12})−DNA(T_{12}) pair are known to be unusual and different from other commonly occurring sequences.[8] Therefore, the above comparison of the OPNA with DNA and PNA may not be extended to other sequences. However, the advantage of the flexible main chain of the OPNA in its high adaptability to form stable double-stranded form is very clearly demonstrated in this case.

The sequence specificity of the OPNA was examined by using DNA(T_6CT_5), instead of DNA(T_{12}) as the counterpart. The melting curves for the OPNA(A_{12}), DNA(A_{12}), and PNA(A_{12}), respectively, mixed with DNA(T_6CT_5) were measured, and the results of the thermodynamic analysis are listed in Table 1. In the cases of both OPNA and PNA, the transition temperatures were lowered by 13° from those of the complementary pairs. In the case of OPNA, the decrease of T_m is on the same order as the temperature range of the 5−95% transition (15°), indicating that OPNA can detect even a single mismatch. In the case of PNA, however, the decrease of T_m is about half of the temperature range, suggesting that the detection of single mismatch is difficult in this case.

To conclude, the OPNA has improved solubility and shows all-or-none-type hybridization with the complementary DNA and high sequence specificity. These characteristics make the OPNAs promising antisense molecules for medicinal uses.

Acknowledgment. The authors are grateful to Professor Naomichi Baba and Dr. Shinji Toyota for measuring mass spectroscopy.

Supporting Information Available: Experimental details of the synthesis of the δ-amino acid carrying adeninyl base and the OPNA-(A_{12}) (7 pages, print/PDF). See any current masthead page for ordering information and Web access instructions.

JA9820386

(7) (a) Borer, P. N.; Dengler, B.; Tinoco, I., Jr.; Uhlenbeck, O. C. *J. Mol. Biol.* **1974**, *86*, 843. (b) Freier, S. M.; Burger, M. D.; Alkema, D.; Nelson, T.; Turner, D. *Biochemistry* **1983**, *22*, 6198.

(8) (a) Peck, L. J.; Wang, J. C. *Nature* **1981**, *292*, 375. (b) Rhodes, D.; Klug, A. *Nature* **1981**, *292*, 378. (c) Nelson, H. C. M.; Finch, J. T.; Luisi, B. F.; Klug, A. *Nature* **1987**, *330*, 221.